

**This is a self-archived version of an original article. This version may differ from the original in pagination and typographic details.**

**Author(s):** Kankainen, Anu; Novikov, Yuri; Oinonen, M.; Batist, L.; Elomaa, Viki-Veikko; Eronen, Tommi; Hakala, Jani; Jokinen, Ari; Karvonen, Pasi; Reponen, Mikael; Rissanen, Juho; Saastamoinen, Antti; Vorobjev, Gleb; Weber, Christine; Äystö, Juha

**Title:** Isomer and decay studies for the rp process at IGISOL

**Year:** 2012

**Version:** Accepted version (Final draft)

**Copyright:** © SIF, Springer-Verlag Berlin Heidelberg 2012

**Rights:** In Copyright

**Rights url:** <http://rightsstatements.org/page/InC/1.0/?language=en>

**Please cite the original version:**

Kankainen, A., Novikov, Y., Oinonen, M., Batist, L., Elomaa, V.-V., Eronen, T., Hakala, J., Jokinen, A., Karvonen, P., Reponen, M., Rissanen, J., Saastamoinen, A., Vorobjev, G., Weber, C., & Äystö, J. (2012). Isomer and decay studies for the rp process at IGISOL. In J. Äystö, T. Eronen, A. Jokinen, A. Kankainen, I. Moore, & H. Penttilä (Eds.), *Topical collection: An IGISOL Portrait - Selected contributions* (48, pp. 49). Springer. *European Physical Journal A*.  
<https://doi.org/10.1140/epja/i2012-12049-x>

# Isomer and decay studies for the $rp$ process at IGISOL

A. Kankainen<sup>1a</sup>, Yu. N. Novikov<sup>2</sup>, M. Oinonen<sup>3</sup>, L. Batist<sup>2</sup>, V.-V. Elomaa<sup>1b</sup>, T. Eronen<sup>1c</sup>, J. Hakala<sup>1</sup>, A. Jokinen<sup>1</sup>, P. Karvonen<sup>1</sup>, M. Reponen<sup>1</sup>, J. Rissanen<sup>1</sup>, A. Saastamoinen<sup>1</sup>, G. Vorobjev<sup>4</sup>, C. Weber<sup>1d</sup>, and J. Äystö<sup>1</sup>

<sup>1</sup> Department of Physics, University of Jyväskylä, P.O. Box 35, FI-40014 University of Jyväskylä, Jyväskylä, Finland

<sup>2</sup> Petersburg Nuclear Physics Institute, 188300 Gatchina, Russia

<sup>3</sup> Dating Laboratory, P.O. Box 64, FI-00014 University of Helsinki, Finland

<sup>4</sup> Gesellschaft für Schwerionenforschung mbH, Planckstrasse 1, D-64291 Darmstadt, Germany

Received: date / Accepted: date

**Abstract.** This article reviews the decay studies of neutron-deficient nuclei within the mass region  $A = 56 - 100$  performed at the Ion Guide Isotope Separator On-Line (IGISOL) facility in the University of Jyväskylä over last 25 years. Development from He-jet measurements to on-line mass spectrometry, and eventually to atomic mass measurements and post-trap spectroscopy at IGISOL, has yielded studies of around 100 neutron-deficient nuclei over the years. The studies form a solid foundation to astrophysical  $rp$ -process path modelling. The focus is on isomers studied either via spectroscopy or via Penning-trap mass measurements. The review is complemented with recent results on the ground and isomeric states of  $^{90}\text{Tc}$ . The excitation energy of the low-spin isomer in  $^{90}\text{Tc}$  has been measured as  $E_x = 144.1(17)$  keV with JYFLTRAP double Penning trap and the ground state of  $^{90}\text{Tc}$  has been confirmed to be the  $(8^+)$  state with a half-life of  $T_{1/2} = 49.2(4)$  s. Finally, the mass-excess results for the spin-gap isomers  $^{53}\text{Co}^m$  and  $^{95}\text{Pd}^m$  and implications from the JYFLTRAP mass measurements for the  $(21^+)$  isomer in  $^{94}\text{Ag}$  are discussed.

**PACS.** 23.40.-s Beta decay – 21.10.-k Properties of nuclei; nuclear energy levels

## 1 Introduction

Decay studies of neutron-deficient nuclides have a long tradition in the IGISOL group in Jyväskylä. Even before the era of the ion-guide method, several studies had been performed with the helium-jet technique at the MC-20 cyclotron in Jyväskylä. Those studies included the  $T_Z = -1$  beta-delayed proton/alpha emitters  $^{20}\text{Na}$  [1],  $^{24}\text{Al}$  [2],  $^{24}\text{Al}^m$  [2],  $^{28}\text{P}$  [3],  $^{32}\text{Cl}$  [3],  $^{36}\text{K}$  [4],  $^{40}\text{Sc}$  [5] as well as the mirror nuclei  $^{49}\text{Mn}$  [6],  $^{53}\text{Co}$  [6], and  $^{59}\text{Zn}$  [7]. After the invention of the new ion-guide method [8], these decay studies were continued at IGISOL and focused on the  $T_Z = -1/2$  mirror nuclei  $^{43}\text{Ti}$  [6],  $^{51}\text{Fe}$  [9], and  $^{55}\text{Ni}$  [9].

After commissioning of the K-130 cyclotron, another milestone in the decay studies of neutron-deficient nuclides has been the application of the heavy-ion ion-guide HIGISOL in the production of these nuclides [10, 11]. Previously, the ions of interest had been produced by light

ion ( $p$  or  $^3\text{He}$ ) fusion-evaporation reactions, which limited the studies close to the stability line. With HIGISOL, the heavy-ion fusion-evaporation reactions became available, and a broader range of radioactive isotopes could be studied in the heavier mass region.

The third major step forward has been the application of the JYFLTRAP Penning trap mass spectrometer for the mass measurements of neutron-deficient nuclides at IGISOL. This has also made it possible to measure the excitation energies of the isomers very precisely. JYFLTRAP has also been used for isobarical, and in some cases, isomeric purification of the IGISOL beams. The mass measurements of neutron-deficient nuclides are reviewed in another article in this special issue of Hyperfine Interactions.

We hope that this contribution provides a view to the history, presence and opportunities of the ion guide-related methodology in studying neutron-deficient nuclei beyond the doubly-magic  $^{56}\text{Ni}$ . In the following sections, decay studies of mirror nuclei and the isospin triplet at  $A = 58$  will be discussed at first. Then, the mass region around  $A = 80 - 90$  rich of isomers is discussed with the main focus on the isomers. In addition, the three spin-gap isomers studied at JYFLTRAP are reviewed in Sect. 4. The investigated nuclides lie on the path of the astrophysical rapid proton capture ( $rp$ ) process, a sequence of proton captures and  $\beta^+$  decays occurring at high temper-

<sup>a</sup> Email: anu.k.kankainen@jyu.fi

<sup>b</sup> Present address: Turku PET Centre, Accelerator Laboratory, Åbo Akademi University, FI-20500 Turku, Finland

<sup>c</sup> Present address: Max-Planck-Institut für Kernphysik, Saupfercheckweg 1, D-69117 Heidelberg, Germany

<sup>d</sup> Present address: Department of Physics, Ludwig-Maximilians-Universität München, D-85748 Garching, Germany

atures and hydrogen densities, such as in X-ray bursts [12, 13] (see Fig. 1). The  $rp$  process has been one motivation for these studies as the detailed knowledge of beta decays, half-lives, energy levels and isomers of the involved nuclides is required for an accurate modeling of the process. Long-lived isomers could play a role by increasing the reaction flow and thus reducing the timescale for the  $rp$ -process nucleosynthesis during the cooling phase [14].

## 2 Decay studies of isospin doublets and the $A = 58$ triplet

### 2.1 $T_Z = -1/2$ mirror nuclei

Mirror nuclei offer an interesting possibility to study the Gamow-Teller (GT) strength in fast mixed Fermi and GT transitions between the ground states of these nuclei. Since the Fermi strength is constant in these mirror transitions, the Gamow-Teller matrix element of the transition can be extracted and compared to the strength obtained from shell-model calculations. A persistent quenching of the GT strength has been observed and quenching factors of 0.744(15) [20] and 0.77(2) [21] have been determined for the  $pf$  and  $sd$  shells, respectively.

At IGISOL, beta-decay study of  $^{55}\text{Ni}$  was one of the first experiments performed with the ion-guide method [9]. There, a 27-MeV  $^3\text{He}$  beam on enriched  $^{54}\text{Fe}$  target was applied from the old MC-20 cyclotron to produce  $^{55}\text{Ni}$ . With a beta telescope, an endpoint energy of 7.70(18) MeV and a half-life of 208(5) ms were determined [9]. The  $\gamma$  spectrum was recorded with a 19 % Ge(Li) detector but no feeding to other states than the ground state was observed. Also the beta decay of  $^{51}\text{Fe}$  produced with the same beam on  $^{50}\text{Cr}_2\text{O}_3$  target was studied with the same setup. The obtained half-life and the endpoint energy were 310(5) ms and 7.26(15) MeV [9], respectively. A beta feeding of 5.0(13) % to a  $7/2^-$  state at 237 keV was determined from the intensity ratio to the annihilation peak [9]. Ion-guide method was also used for a half-life determination of  $^{43}\text{Ti}$  with a beta telescope [6]. The ions of interest were produced via  $^{40}\text{Ca}(\alpha, n)^{43}\text{Ti}$  reactions with an 18-MeV alpha beam from the MC-20 cyclotron. The measured half-life was 509(5) ms [6].

### 2.2 $T = 1$ triplet at $A = 58$

In addition to beta decays, Gamow-Teller strength can be studied via charge-exchange (CE) reactions. The CE reactions, such as  $^{58}\text{Ni}(^3\text{He}, t)^{58}\text{Cu}$  [22], are not limited by the  $Q$  value as beta-decay strength studies, and thus, GT strengths over a broader energy range can be investigated. However, the charge-exchange reactions rely on the proportionality between the cross section near  $0^\circ$  scattering angle and the GT strength. This proportionality has to be normalized, for example at  $A = 58$  with the GT strength value from the beta decay of  $^{58}\text{Cu}$ .

In order to provide a more precise value for the normalization, beta decay of  $^{58}\text{Cu}$  was measured at IGISOL.

About 4000 ions/s of  $^{58}\text{Cu}$  were produced at IGISOL with an 18-MeV, 15- $\mu\text{A}$  proton beam from the K-130 cyclotron impinging on an enriched  $^{58}\text{Ni}$  target [23]. At the implantation point, the yield of  $^{58}\text{Cu}$  and corresponding  $\gamma$  transitions were monitored by two HPGe detectors and a plastic  $\Delta E_\beta$  detector. The tape was moved to the measurement position, where the ratio of the intensities of the 511-keV annihilation radiation to the 1454-keV  $\gamma$  transition in  $^{58}\text{Ni}$  was precisely measured. A branching ratio of 80.8(7) % to the  $^{58}\text{Ni}$  ground state was obtained [23].

Recently, a  $Q_{\text{EC}}$  value for the beta decay of  $^{58}\text{Cu}$  has been precisely determined at JYFLTRAP [18]. When this new  $Q_{\text{EC}}$  value is combined with the branching ratio of 81.1(4) % (from the values of 80.8(7) % [23], 81.2(5) % [24] and 82(3) % [25]) and a half-life of 3.204(7) s [26] for  $^{58}\text{Cu}$ , a Gamow-Teller strength  $B(GT) = 0.08285(46)$  and a squared Gamow-Teller matrix element  $\langle\sigma\tau\rangle^2 = 0.05141(33)$  are obtained. The values are little higher and more precise than previously (c.f.  $B(GT) = 0.0821(7)$  and  $\langle\sigma\tau\rangle^2 = 0.0512(5)$  in Ref. [23]).

The  $T = 1$  triplet at  $A = 58$  offers a possibility to study the isospin symmetry of transitions. Namely, the Gamow-Teller strength to the states in  $^{58}\text{Cu}$  obtained from the ( $^3\text{He}, t$ ) charge-exchange reactions on  $^{58}\text{Ni}$  ( $T_Z = +1$ ) [22] can be compared with the strengths of the analogous transitions from the beta decay of  $^{58}\text{Zn}$  ( $T_Z = -1$ ). For this purpose, beta-decay of  $^{58}\text{Zn}$  has been studied with a beta-delayed gamma and proton setups at ISOLDE and at IGISOL [27]. At ISOLDE, the earlier results [28] concerning the half-life and two lowest  $\gamma$  transitions were confirmed. No beta-delayed protons were observed with the ISOLDE Silicon Ball detector [29] similarly to the previous work [28]. Therefore, the experiment was also tried at IGISOL with a 50-MeV, 1- $\mu\text{A}$   $^3\text{He}$  beam on a  $^{\text{nat}}\text{Ni}$  target. The estimated yield of  $^{58}\text{Zn}$  at IGISOL was about 0.6 atoms/s based on the 203-keV  $\gamma$  transition [30]. Unfortunately, no beta-delayed protons were observed at IGISOL either.

## 3 Studies around $A = 80 - 90$ for the $rp$ process

### 3.1 Yttrium isotopes: $^{80}\text{Y}^{\text{m}}$ , $^{81}\text{Y}$ , and $^{82}\text{Y}$

#### $^{80}\text{Y}^{\text{m}}$

$^{80}\text{Y}$  has a long-lived isomeric state at 228.5 keV relevant for the astrophysical  $rp$  process. Since the spin assignment and internal conversion coefficient were not certain, an experiment aiming for the spin identification of this isomer was performed at HIGISOL [10, 11] by employing a 150-MeV  $^{32}\text{S}^{7+}$  beam on a 2.7 - mg/cm<sup>2</sup>-thick  $^{54}\text{Fe}$  target [31]. The isomeric transition was studied with a magnetic conversion electron transporter spectrometer ELLI [32] and a low-energy Ge detector (LeGe). ELLI transported electrons from the implantation point to a cooled Si(Au) surface barrier detector in a remote detection area, which helped to reduce the background. The observed

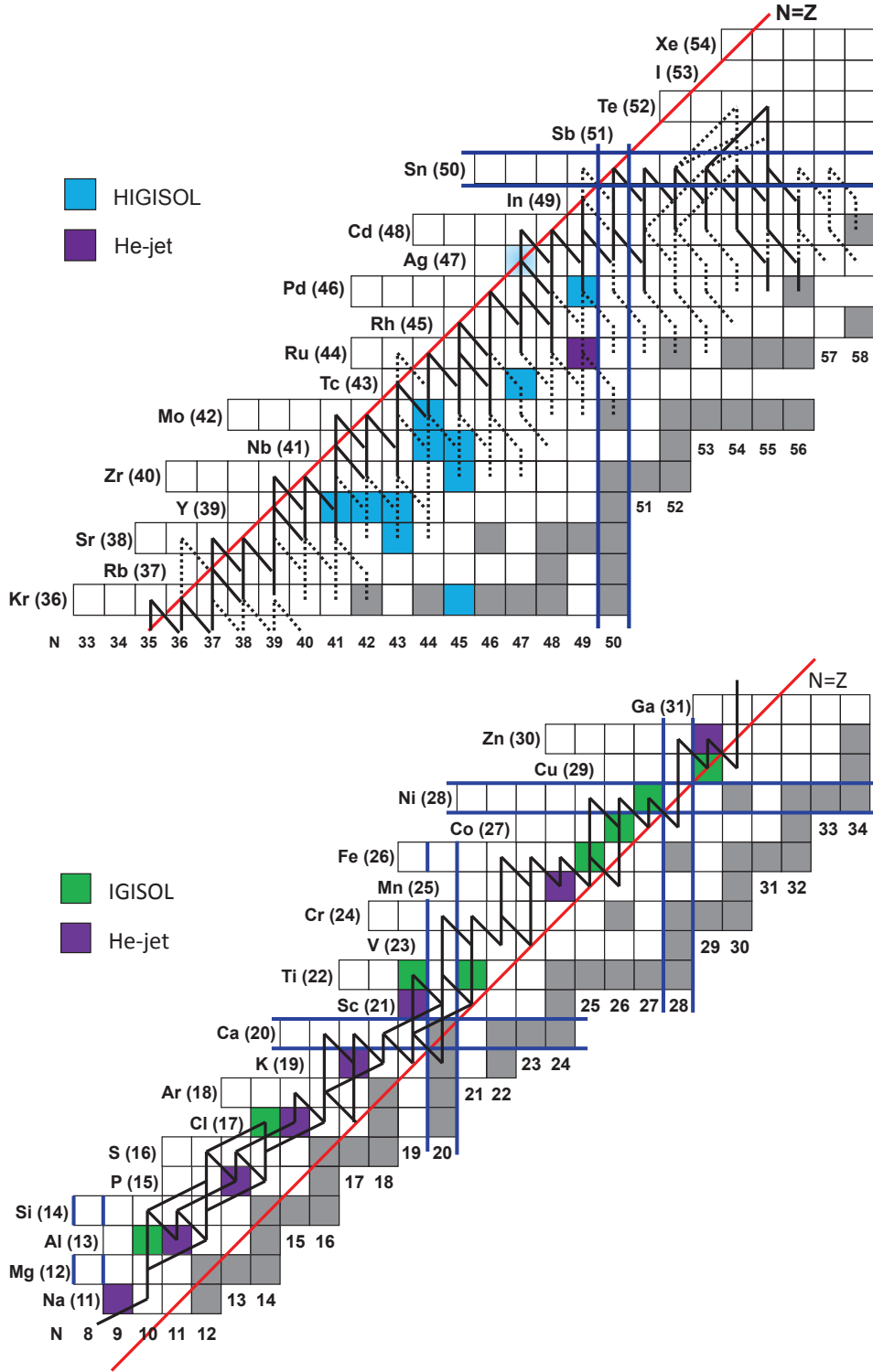


**Fig. 1.** Nuclides studied via beta-decay spectroscopy with He-jet, IGISOL and HIGISOL techniques in Jyväskylä. For the lower mass region, the main path of the  $rp$  process is drawn for one-zone X-ray burst model according to Ref. [15]. For the higher mass region, the time-integrated reaction flow has been plotted for conditions where the thermonuclear burning proceeds in steady-state [16]. There, the solid line represents the major path (more than 10 % of the reaction flow through  $3\alpha$  reaction) and the dashed line the minor path (1 – 10 % of the reaction flow through  $3\alpha$  reaction). Recent mass measurements at JYFLTRAP [17] have shown that the SnSbTe cycle is not so strong as plotted here.  $^{53}\text{Co}$  has been studied both with the He-jet technique [6] and with JYFLTRAP at IGISOL [18]. The energy of the spin-gap isomer in  $^{94}\text{Ag}$  has been estimated based on JYFLTRAP mass measurements. Decay studies of  $^{23}\text{Al}$ ,  $^{31}\text{Cl}$ , and  $^{41}\text{Ti}$  are discussed in a separate article [19].

228.5-keV  $\gamma$ -rays were not in coincidence with the beta particles. Moreover, the coincidence of yttrium  $K_\alpha$  X-rays with the 228.5-keV transition confirmed the isomeric character. The internal conversion coefficient for the isomeric transition was determined from the ratio of the conversion electrons to the corresponding  $\gamma$ -rays as well as from the ratio of yttrium  $K$  X-rays to the 228.5-keV  $\gamma$ -rays. The contribution from the beta decay of  $^{80}\text{Zr}$  to the yttrium X-rays is negligible since the production rate of  $^{80}\text{Zr}$  is very small. The obtained values  $\alpha_K = 0.51(9)$  [31] and  $\alpha_K = 0.48(13)$  [31] agree well with each other and with the result of Ref. [33],  $\alpha_K = 0.47(15)$ . The average value of  $\alpha_K = 0.50(7)$  [31] gives  $M3 + (E4)$  multipolarity for the 228.5-keV transition and a spin assignment  $1^-$  for the isomer.

The measured half-life of the isomeric transition,  $T_{1/2} = 5.0(5)$  s [31], is in agreement with the previous result of  $T_{1/2} = 4.7(3)$  s [34]. The weighted mean for the half-life of the 228.5-keV isomeric transition is  $T_{1/2} = 4.8(3)$  s, which converts into a bare half-life of  $T_{1/2} = 6.8(5)$  s [31] corresponding the fully ionized  $^{80}\text{Y}^m$  in the stellar plasma of an X-ray burst. In the  $rp$  process,  $^{80}\text{Y}^m$  is produced via beta decay of  $^{80}\text{Zr}$  which dominantly populates the  $(1^+)$  states at 623 keV and at higher energies [35]. De-excitations of these states lead finally to the 228.5-keV  $1^-$  isomeric state. About 19(2) % of the isomeric decays proceed via beta decay and the rest 81(2) % via internal transition to the  $^{80}\text{Y}$  ground state [36]. Since the decay of the isomeric state is many orders of magnitudes slower than the proton captures on it during most of the  $rp$  process, the proton captures will predominantly occur on the isomeric state [31] and not on the ground state of  $^{80}\text{Y}$  as previously assumed. This is a clear example how isomers can play a role in the  $rp$  process and should be known for an accurate modeling.

### $^{81}\text{Y}$

$^{81}\text{Y}$  was produced at HIGISOL with a 150-170 MeV  $^{32}\text{S}^{7+}$  beam impinging on an enriched  $^{54}\text{Fe}$  (1.8 mg/cm<sup>2</sup>) target [37]. Beta-decay of  $^{81}\text{Y}$  was studied at HIGISOL with a setup consisting of two HPGe detectors, a LeGe detector and the magnetic conversion-electron transporter spectrometer ELLI [32]. Before this HIGISOL experiment [37], beta-decay of  $^{81}\text{Y}$  had been studied already in Refs. [38–40]. All known  $\gamma$  transitions [41] following the beta decay of  $^{81}\text{Y}$  could be observed at HIGISOL except the 216.6-keV transition. Conversion electrons from the 43.2-, 79.23-, 101.05-, 115.39-, 124.16-, and 155.20-keV transitions in  $^{81}\text{Sr}$  were measured. The internal conversion coefficient for the 43.2-keV transition was determined as  $\alpha_K = 1.5(3)$ , which supports an  $M1 + E2$  multipolarity for the transition [37]. The obtained low conversion coefficient ( $\alpha_K = 0.03(1)$ ) for the 124-keV transition supports an  $E1$  multipolarity for the transition. The measured conversion coefficient for the 79.23-keV transition,  $\alpha_K = 2.3(1)$ , agrees nicely with the literature value of 2.3(6) [39], and supports an  $E2$  multipolarity. Figure 2 shows an example

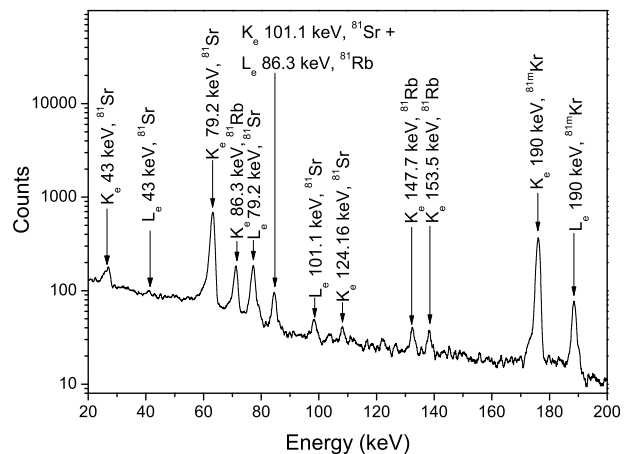


**Fig. 2.** Conversion electron spectrum measured at  $A = 81$  with the magnetic conversion-electron transporter spectrometer ELLI [32] at IGISOL.

of conversion electron spectrum measured with ELLI at  $A = 81$ .

### $^{82}\text{Y}$

$^{82}\text{Y}$  was produced at HIGISOL using the reaction  $^{165}\text{MeV } ^{32}\text{S} + ^{\text{nat}}\text{Ni}$  [10]. A 37 % Ge detector was used for detecting  $\gamma$ -rays, a LeGe detector for X-rays and a 1-mm plastic scintillator for detecting beta particles [10]. Beta-decay of  $^{82}\text{Y}$  had been studied via  $^{60}\text{Ni}(^{24}\text{Mg}, \text{pn})^{82}\text{Y}$  and  $^{60}\text{Ni}(^{28}\text{Si}, \alpha \text{pn})^{82}\text{Y}$  reactions with beam energies of 90 and 110 MeV [38] and via  $^{54}\text{Fe}(^{32}\text{S}, 3\text{pn})^{82}\text{Y}$  reaction at an energy of 123 MeV [39]. The measured half-lives of 9.5(4) s [38] and 9.5(5) s [39] agree with each other but the values for the relative intensity of the 602-keV  $\gamma$ -transition, 41 % [38] and 13(1) % [39], differ a lot. At HIGISOL, the half-life was determined from the beta particles, annihilation  $\gamma$ -rays, as well as from the 573, 602, 737, 1176 and 1291 keV  $\gamma$ -transitions following the beta-decay of  $^{82}\text{Y}$  [10]. The shorter-lived  $^{82}\text{Zr}$  might distort the half-lives obtained from the beta particles and from the annihilation radiation, and since the measured half-life values of  $^{82}\text{Zr}$  vary a lot, the value of 8.30(20) s based on the most intensive, 573-keV  $\gamma$  transition was adopted [10]. The statistics of the other  $\gamma$  transitions were too poor for precise half-life fitting. The half-life measured at HIGISOL disagrees with the former values of [38,39] but is much more precise.

The obtained relative intensity of 4.4(4) % [10] for the 602-keV transition deviates from the previous He-jet studies [38,39]. In the He-jet studies no mass separation is used and contamination for example from the 602-keV  $\gamma$ -transitions following the beta decay of  $^{84}\text{Y}$ , ( $6^+$ ) state, cannot be excluded. Therefore, the obtained relative intensities for the 602-keV transition in [38,39] can be higher than at HIGISOL, where a clear spectrum at mass  $A = 82$  was obtained.

The mass of  $^{82}\text{Y}$  has been measured precisely with the JYFLTRAP Penning trap mass spectrometer [42]. The difference to the Atomic Mass Evaluation 2003 (AME03)

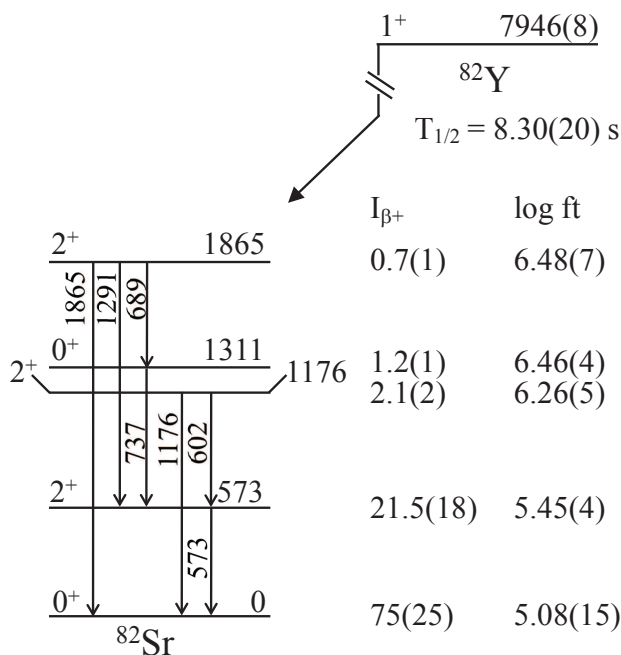


**Fig. 3.** Proposed decay scheme of Ref. [10] revised with the  $Q_{EC}$  value from Ref. [42].

[43] value is 127(100) keV. The updated  $Q_{EC}$  value for  $^{82}\text{Y}$  is 7946(8) keV, which is 130 keV higher and 13 times more precise than in the AME03. The updated  $\log ft$  values of the  $^{82}\text{Y}$  beta decay are little higher than previously (see Fig. 3).

Neutron-deficient yttrium isotopes have typically isomers. No clear evidence for an existence of an isomer in  $^{82}\text{Y}$  with a significantly different half-life than the  $1^+$  ground state was observed in Ref. [10]. On the other hand, for example the production of  $^{84}\text{Y}$  was found to be almost totally concentrated on the  $5^-$  39.5-min isomeric state: only about 1 % of the  $^{84}\text{Y}$  production was due to the  $1^+$  ground state based on the intensities of the 793-keV and 974-keV  $\gamma$ -transitions [10].

### 3.2 Niobium isotopes: $^{85}\text{Nb}^m$ and $^{86}\text{Nb}$

#### $^{85}\text{Nb}^m$

A 37 % Ge detector for detecting  $\gamma$ -rays, a LeGe detector for X-rays and a 1-mm plastic scintillator for detecting beta particles were employed in a spectroscopic survey at  $A = 85$  carried out at HIGISOL by using 165-MeV  $^{32}\text{S} + ^{\text{nat}}\text{Ni}$  reactions [10]. Several unknown  $\gamma$ -rays were found with energies of 166, 272, 423, 434, 484, 532, 538, 590, 610, 660, 709, and 759 keV at  $A = 85$ . The most intense, 759-keV  $\gamma$  transition had a half-life of 12(5) s agreeing with the beta-decay half-life of  $^{85}\text{Zr}^m$  ( $T_{1/2} = 10.9(3)$  s [44]), and disagreeing with the half-lives of  $^{85}\text{Mo}$  ( $T_{1/2} = 3.2(2)$  s [45]) and  $^{85}\text{Nb}$  ( $T_{1/2} = 20.9(7)$  s [46]). However, the transition could not be associated with the beta decay of  $^{85}\text{Zr}^m$  since such an intense transition should have been observed in the detailed beta-decay study of Ref. [47]. At

HIGISOL, only the two most intensive peaks at 416 and 454 keV following the  $^{85}\text{Zr}$  beta decay were observed. The half-life for the unknown 484-keV transition was determined as  $T_{1/2} = 4_{-2}^{+8}$  s [10] consistent with the reported half-life of  $^{85}\text{Mo}$ . This transition could not be associated with the beta decays of  $^{85}\text{Nb}$  and  $^{85}\text{Zr}$  due to the different half-lives. Similarly to the 759-keV transition, the 484-keV transition should have been detected in Ref. [47] if it was associated with the  $^{85}\text{Zr}^m$ . As a summary, the 759-keV, 12(5) s transition follows either the beta decay of  $^{85}\text{Nb}^m$  or  $^{85}\text{Mo}^m$ . In addition to the isomer in Nb or Mo, the 484-keV transition could originate from the beta decay of  $^{85}\text{Mo}$ .

Unknown  $\gamma$ -rays at energies of 272, 484, 530, 536, 590, 660, 709, and 758 keV were also observed with two HPGe detectors at the implantation point in a run employing a 150–170-MeV  $^{32}\text{S}^{7+}$  beam on a  $^{\text{nat}}\text{Ni}$  target at HIGISOL [37]. After 15 or 40 seconds, the activity was moved to the LeGe detector station. There, none of these  $\gamma$ -rays could be observed supporting short half-lives for these transitions. It should also be noted that about half of the observed 12 unknown  $\gamma$ -transitions in Ref. [10] at  $A = 85$  have an energy difference of 50 keV:  $484 - 434 = 50$  keV,  $660 - 610 = 50$  keV and  $759 - 709 = 50$  keV. In addition, the differences  $532 - 484 = 48$  keV and  $590 - 538 = 52$  keV are quite close to 50 keV which corresponds to the energy of a well-known 50-keV transition in  $^{85}\text{Zr}$ . One possibility is that these  $\gamma$ -rays follow the beta decay of an isomer in  $^{85}\text{Nb}$  to the possible states at 484 keV, 660 keV and 759 keV (and possibly at 590 keV), which de-excite to the  $(7/2^+)$  ground state and to the  $(7/2^+, 9/2^+)$  state at 50 keV in  $^{85}\text{Zr}$ . However, no coincidences have been checked between these  $\gamma$ -rays or between the Zr, Nb or Mo X-rays and these transitions. Thus, we cannot conclude to which nucleus these transitions belong. Trap-assisted spectroscopy at  $A = 85$  would enlighten the situation provided the yields are high enough.

In the latter run at  $A = 85$  [37], conversion electrons at 32.1 and 50 keV were observed with ELLI. The 32.1-keV conversion electrons were in coincidence with Zr  $K$  X-rays, thus confirming that they belong to the 50-keV transition in  $^{85}\text{Zr}$ . The determined internal conversion coefficient for the 50-keV transition,  $\alpha_K = 1.7(2)$ , suggests a mixed  $M1 + E2$  multipolarity for the transition. The half-life determined for this 50-keV transition fed by the beta decay of  $^{85}\text{Nb}$  was 17(2) s, which is little shorter than  $T_{1/2} = 20.9(7)$  s given for  $^{85}\text{Nb}$  in Ref. [46].

The 50-keV conversion electrons were in coincidence with the Nb  $K$  X-rays and had a half-life of 3.3(9) s. Since the electrons were not in coincidence with beta particles and because the production rate of  $^{85}\text{Mo}$  is much smaller than for  $^{85}\text{Nb}$ , we identify this transition as a 69-keV isomeric transition in  $^{85}\text{Nb}$ . Based on the internal conversion coefficients, the preferred multipolarity for the transition would be  $E2$  or  $M2$ , which would mean a much shorter half-life than 3.3 s. An indication of beta-decay of this isomer to the 292-keV isomeric state in  $^{85}\text{Zr}$  is observed in the time behaviour of the 292-keV  $\gamma$ -line [37].

At JYFLTRAP, the  $Q_{EC}$  value of  $^{85}\text{Nb}$  has been measured as 6898(9) keV [42] which is 900(200) keV higher than the previous value [46]. There, the beta-endpoint energy was determined from the beta spectrum in coincidence with the 50-keV transition in  $^{85}\text{Zr}$ . If the 50-keV transition is fed by de-excitations from possible states at 484 keV, 660 keV and 759 keV in  $^{85}\text{Zr}$ , this would increase the deduced  $Q_{EC}$  value of Ref. [46] and move it closer to the JYFLTRAP value. Although the beta-decay experiments tend to underestimate  $Q_{EC}$  values, such a big difference suggests that it should be verified for which state the mass of  $^{85}\text{Nb}$  has been measured. For example, a half-life measurement using the isobarically purified beta emitters after JYFLTRAP would allow us to distinguish between the 20.9-s ground state and the suggested isomers with half-lives of 3.3(9) s [37] and 12(5) s [10].

### $^{86}\text{Nb}$

$^{86}\text{Nb}$  has a ( $6^+$ ) ground state with a half-life of 88(1) s and a suggested high-spin isomer with a half-life of 56(8) s [48]. In the HIGISOL run employing a 150 – 170 MeV  $^{32}\text{S}^{7+}$  beam on a  $^{nat}\text{Ni}$  target [37], accumulation times of 40 s and 200 s were used for  $A = 86$ . There,  $\gamma$  peaks at energies of 47.7, 50.1, 97.8 and 186.8 keV following the beta decay of the  $0^+$  ground state of  $^{86}\text{Mo}$  were observed [37]. These low-spin states in  $^{86}\text{Nb}$  are located at the energies of  $E_0$ ,  $E_0 + 50.1$  keV,  $E_0 + 97.8$  keV, and  $E_0 + 236.9$  keV. Multipolarities for the  $\gamma$  transitions have been determined and they are most likely  $E1$  except  $M1$  for the 47.7-keV transition. A half-life of 19.1(3) s for  $^{86}\text{Mo}$  was determined from the time behaviour of  $\gamma$ , Nb  $K$  X-ray, and electron peaks [37]. This is in agreement with the value of 19.6(11) s obtained in Ref. [48]. No evidence for the 56-s isomer was found in Ref. [37]. No converted low-energy transitions with an energy  $E_0$  were observed. Thus, the lowest low-spin state  $E_0$  fed by the  $^{86}\text{Mo}$  beta decay, should be either highly excited or decay mainly via beta decay to  $^{86}\text{Zr}$ .

At JYFLTRAP, the mass-excess value of  $^{86}\text{Nb}$  [37] was found to be 700(90) keV higher than in the AME03 [43]. Here, again, the ground-state nature of the measured mass should be verified for example via half-life determination after the trap. In addition, the production ratio of the isomer to ground state at HIGISOL can shed light on which mass has been measured.

### 3.3 $^{90}\text{Tc}^m$

The beta decay of  $^{90}\text{Tc}$  has been studied in Refs. [49] and [50]. A  $1^+$  state with a half-life of 8.7(2) s and a high-spin state ( $6^+$ ) with a half-life of 49.2(4) s were found in Ref. [50]. The corresponding excitation energy of the suggested ( $6^+$ ) isomer has been estimated to be 124(390) keV [51]. In Ref. [52], the ground state was suggested to be an  $8^+$  state based on the systematics of all neighbouring  $N = 47, 49$  nuclei. In a study of the  $^{90}\text{Ru}$   $0^+$  ground-state beta decay [53], feeding to three low-spin states in  $^{90}\text{Tc}$  was found. There, a high-spin  $8^+$  ground state was

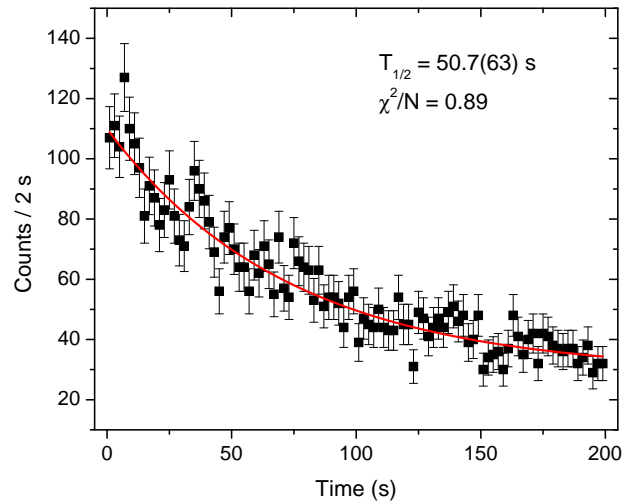


**Fig. 4.** One-component fit on the time behaviour of the beta particles at  $A = 90$  measured after the IGISOL dipole magnet.

obtained, when the low-spin and high-spin results of shell-model calculations were compared to the experimental results.

$^{90}\text{Tc}$  has been studied previously at HIGISOL via a JYFLTRAP mass measurement [51]. There, the measured mass excess was assigned for the  $8^+$  ground state. Since the identification of the ground or isomeric state is uncertain, a new experiment was performed with a  $^{40}\text{Ca}^{8+}$  beam on a  $^{nat}\text{Ni}$  target at 210 MeV. In that experiment, a half-life for the mass  $A = 90$  was determined by measuring the time behaviour of beta particles with a Silicon detector after the IGISOL dipole magnet. A half-life of  $T_{1/2} = 50.7(63)$  s was obtained with a one-component fit (see Fig. 4). This is in agreement with the half-life of the high-spin state ( $8^+$ ),  $T_{1/2} = 49.2(4)$  s [50] and shows that the contribution from the low-spin  $1^+$ , 8.7(2)-s state [50] is small. The half-lives of  $^{90}\text{Nb}$  (14.60(5) h [54]) and  $^{90}\text{Mo}$  (5.56(9) h [54]) can be considered to be constant within the time scale of 200 s.  $^{90}\text{Ru}$  ( $T_{1/2} = 11(3)$  s) is much less produced than  $^{90}\text{Tc}$  and thus, does not contribute much to the beta-particle time behaviour. The Mo and Nb isomers decay via internal transition and do not contribute to the beta spectrum.

The isomer in  $^{90}\text{Tc}$  was also observed with JYFLTRAP in the experiment employing  $^{40}\text{Ca}^{8+} + ^{nat}\text{Ni}$  at HIGISOL, as shown in Fig. 5. Three measurements of the  $^{90}\text{Tc}$  ground state and five measurements of the isomeric state against the  $^{86}\text{Kr}$  reference were performed with the time-of-flight ion-cyclotron resonance (TOF-ICR) method [55,56]. In the precision trap, a quadrupolar RF excitation time of 800 ms was applied for the ions of interest. In total, there were 14331 ions of  $^{90}\text{Tc}$  and 4229 ions of  $^{90}\text{Tc}^m$  in the analysis. The count-rate class analysis [57] was performed for the ground state with three classes. For the isomer, no count-rate class analysis could be performed. Therefore, the ion number was limited to 1 – 2 ions per bunch in the analysis of the isomeric state. The uncertainty of the cyclotron frequency of the isomer was multiplied by a factor



**Table 1.** Measured frequency ratios and mass excess (ME) values of  $^{90}\text{Tc}$  and  $^{90}\text{Tc}^m$  obtained at JYFLTRAP in this work using  $^{86}\text{Kr}^+$  as a reference. The result for the ground-state mass agrees with the previous experiments at JYFLTRAP (ME =  $-70723.6(39)$  keV) [51] and SHIPTRAP (ME =  $-70724.1(74)$  keV) [51], which employed  $^{85}\text{Rb}^+$  ions as a reference.

Nuclide	$r$	ME (keV)	$E_x$ (keV)
$^{90}\text{Tc}$	1.046717034(13)	$-70724.7(11)$	0
$^{90}\text{Tc}^m$	1.046718834(16)	$-70580.6(13)$	144.1(17)

of two. This was based on a comparison of the non- $Z$ -classified results to the  $Z$ -classified results of the ground state and the reference. The weighted mean of the frequency ratios and the internal and external errors [58] were calculated. The internal errors were bigger than the external errors showing that the fluctuations of the frequency ratios were purely statistical. The mass-dependent and residual uncertainties [59] were added to the measured frequency ratios quadratically. The resulting frequency ratios and mass-excess values are given in Table 1.

When the time-of-flight spectrum for  $^{90}\text{Tc}$  is fitted with two peaks (see Fig. 5.(a)), the fractions of the lower-mass state and the higher-mass state are 89(5) % and 11(5) %, respectively. A very similar result is obtained if a two-component fit is performed to the beta-particle time behaviour at  $A = 90$ : half-lives of 60(21) s and 8(14) s are obtained with fractions of 84(19) % and 16(16) %, respectively. This indicates that the low-spin state is much less produced than the high-spin state at HIGISOL. Thus, we confirm that the previously measured mass excess of  $^{90}\text{Tc}$  really was the mass of the more favorably produced ( $8^+$ ) ground state with a half-life of  $T_{1/2} = 49.2(4)$  s.

The excitation energy obtained for the isomer,  $E_x = 144.1(17)$  keV, fits well with the shell-model prediction of a  $2^+$  state (143 keV [52], 160 keV [53]). However,  $\log ft$  values of around 5 – 6 to the  $0^+$  ground state and to the  $2^+$  state at 948.1 keV in  $^{90}\text{Mo}$  [49,50] support a  $1^+$  assignment. The  $2^+$  assignment is possible if the ground-state feeding has not been correctly determined.

### 3.4 $^{93}\text{Ru}^m$

Beta decay of  $^{93}\text{Ru}^m$  ( $T_{1/2} = 10.8(3)$  s,  $J^\pi = (1/2^-)$ ) has been studied via a 24-MeV  $^3\text{He}$  beam from the University of Jyväskylä MC-20 cyclotron on an isotopically enriched  $^{92}\text{Mo}$  target employing the He-jet technique [61]. The total decay energy of the isomer was measured as 7070(85) keV and the proton binding energy of  $^{93}\text{Tc}$  as 4086.5(10) keV [61]. The excitation energy of the isomer is 734.4(1) keV [62]. The transition was suggested as an isomeric transition in  $^{93}\text{Ru}$  since it was not in coincidence with any other  $\gamma$ -ray or annihilation radiation. Later, in Ref. [53], the beta decay of  $^{93}\text{Rh}$  was studied via the reaction  $^{58}\text{Ni}(^{40}\text{Ar}, p4n)^{93}\text{Ru}$ . There, no evidence for the  $(1/2)^-$  isomeric state in  $^{93}\text{Ru}$  was found. Thus, the low-

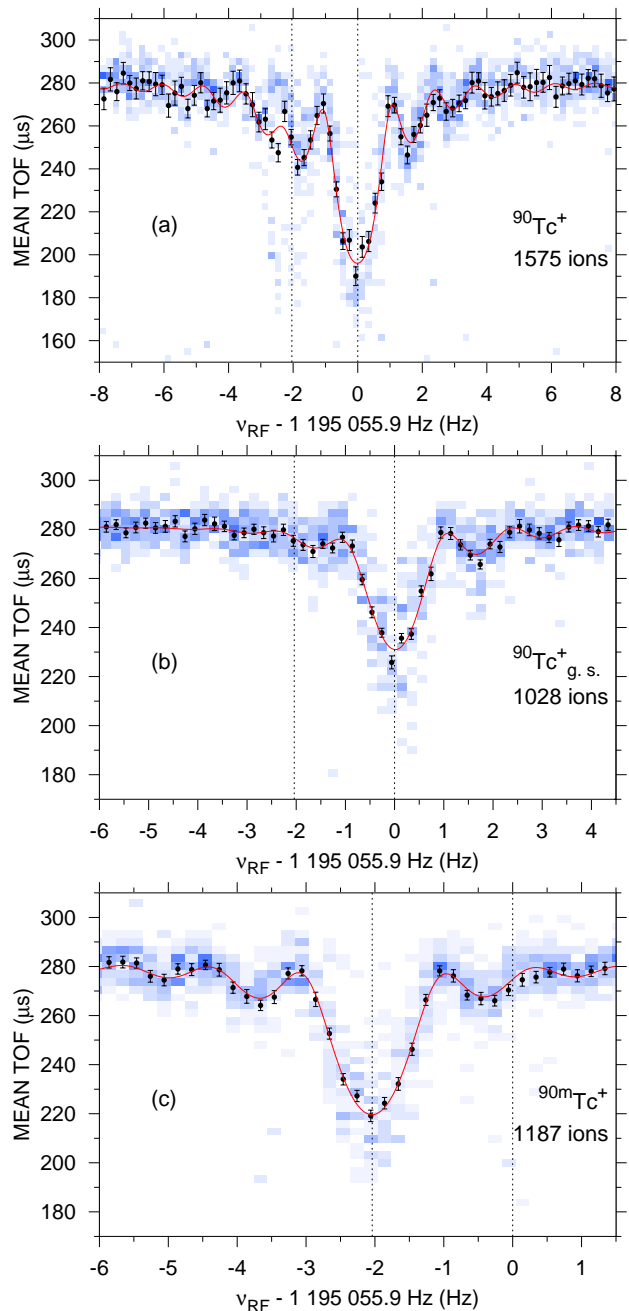


**Fig. 5.** Time of flight spectra after 800 ms quadrupolar rf excitation for (a) both ground and isomeric state in  $^{90}\text{Tc}$ , (b) the ground state  $^{90}\text{Tc}$  and (c) the isomeric state  $^{90}\text{Tc}^m$ . Blue shading around the data points indicates the number of ions in each time-of-flight bin: the darker the bin, the more ions. The isomer contribution is clearly seen in Fig. (a). The dashed lines show the positions of the ground and isomeric states obtained from Figs. (b) and (c). The TOF spectra shown here are based on single files, where the number of ions has been limited to 1 – 2 ions per bunch. The selected time window has been 147.2 – 307.2  $\mu\text{s}$  for the figure (a) and 179.2 – 307.2  $\mu\text{s}$  for (b) and (c). The cleaning method [60] based on electric dipole excitation with time-separated oscillatory fields has been applied in figures (b) and (c).



spin isomeric state is not populated at all or only weakly populated in these kind of reactions.

The mass of  $^{93}\text{Ru}$  has been studied at JYFLTRAP [51] and it agrees with the values of Ref. [61]. The ground state should be well resolved from the isomeric state at 734.4(1) keV. In future, it would be interesting to measure the mass of the isomeric state by using similar reaction as in Ref. [62] at IGISOL. These measurements could have implications for the *rp* process, because such long-lived isomers can play a role in it.

## 4 High-spin isomers

High-lying, high-spin isomers with relatively long half-lives have been observed close to magic shell closures. Examples of high-spin isomers are  $^{52}\text{Fe}^{\text{m}}$  ( $12^+$ ) [63],  $^{53}\text{Fe}^{\text{m}}$  ( $19/2^-$ ) [64], and  $^{53}\text{Co}^{\text{m}}$  ( $19/2^-$ ) [65] near  $N = Z = 28$ ,  $^{94}\text{Ag}^{\text{m}}$  ( $7^+$  and  $21^+$ ) [66,67],  $^{95}\text{Ag}^{\text{m}}$  [68], and  $^{95}\text{Pd}^{\text{m}}$  ( $21/2^+$ ) [69] near  $N = Z = 50$  and  $^{212}\text{Po}^{\text{m}}$  [70] near  $Z = 82$ ,  $N = 126$ . These high-spin isomers are called spin-gap isomers since they lie lower in energy than the intermediate spin states, thus forcing the isomer to decay either via beta-decay, particle emission or a high-multipolarity internal transition. The excitation energies of these high-spin states are lower due to the effective proton-neutron interaction, which favors an aligned proton-neutron pair. In this section, studies on  $^{53}\text{Co}^{\text{m}}$  ( $19/2^-$ ),  $^{94}\text{Ag}^{\text{m}}$  ( $21^+$ ) and  $^{95}\text{Pd}^{\text{m}}$  ( $21/2^+$ ) performed at IGISOL will be reviewed.

### 4.1 $^{53}\text{Co}^{\text{m}}$

The first observation of proton radioactivity was from the high-spin ( $19/2^-$ ) isomer in  $^{53}\text{Co}$  [65,71,72]. This state with a half-life of 247(12) ms [72] is the isobaric analogue state of the ( $19/2^-$ ) isomeric state in its mirror nucleus  $^{53}\text{Fe}$  [64]. The excitation energy of  $^{53}\text{Co}^{\text{m}}$  as determined from the energy of the observed protons, is 3197(29) keV [71,72]. The isomeric state decays mainly via beta decay to its analogue state in  $^{53}\text{Fe}$  - only about 1.5 % decays to  $^{52}\text{Fe}$  via proton decay [72].

In an experiment at the JYFLTRAP mass spectrometer, both the ground and isomeric state of  $^{53}\text{Co}$  could be produced with a 40-MeV proton beam impinging on an enriched 2 mg/cm<sup>2</sup>-thick  $^{54}\text{Fe}$  target [18]. At JYFLTRAP, a Ramsey excitation with a time pattern of 25–150 (wait)–25 ms was applied for  $^{53}\text{Co}$  and its reference  $^{53}\text{Fe}$ . The masses of the ground state and the isomeric state were measured against each other and against the  $^{53}\text{Fe}$  ground state. The obtained mass-excess values were  $-42657.3(15)$  and  $-39482.9(16)$  keV for the ground and isomeric state, respectively [18]. The mass-excess value for the ground state agrees well with the earlier results [43,73]. The mass-excess value of the isomer agrees with the latter proton-decay experiment [72] but deviates from the first experiment [71]. The excitation energy for the ( $19/2^-$ ) isomeric state obtained as a weighted average from the frequency ratio  $^{53}\text{Co}^{\text{m}}-^{53}\text{Co}$  and from the frequency ratios of  $^{53}\text{Co}^{\text{m}}-^{53}\text{Fe}$  and  $^{53}\text{Fe}-^{53}\text{Co}$ , was 3174.3(10) keV [18].

This new value agrees well with the previously adopted value 3197(29) keV [43] but is 29 times more precise. With the  $^{52}\text{Fe}$  mass from Ref. [43], this would correspond to a proton energy of  $E_{\text{p,lab}} = 1530(7)$  keV [18].

Since  $^{53}\text{Co}$  and  $^{53}\text{Co}^{\text{m}}$  were measured against their beta-decay daughter  $^{53}\text{Fe}$  at JYFLTRAP, also  $Q_{\text{EC}}$  values could be determined precisely. The obtained  $Q_{\text{EC}}$  values from the ground and isomeric state of  $^{53}\text{Co}$  to the ground state of  $^{53}\text{Fe}$  were 8288.12(45) keV and 11462.2(12) keV, respectively [18]. These precisely measured mirror decay  $Q_{\text{EC}}$  values are important for an accurate determination of the corrected *ft* value. In addition, a Coulomb energy difference of 133.9(10) keV [18] was obtained for the ( $19/2^-$ ) states in  $^{53}\text{Fe}$  and  $^{53}\text{Co}$ , which improves the adopted value 157(29) keV [43] a lot.

In future, a direct measurement of the proton separation energy of  $^{53}\text{Co}$  at JYFLTRAP would yield a sub-keV value for this separation energy. This, in turn, would give a precise calibration value for proton spectroscopy experiments. In addition, precise mass measurements of  $^{53}\text{Fe}$ ,  $^{53}\text{Fe}^{\text{m}}$  and  $^{52}\text{Fe}^{\text{m}}$  could be considered in future at JYFLTRAP.

### 4.2 $^{94}\text{Ag}^{\text{m}}$

Two high-spin states, ( $7^+$ ) and ( $21^+$ ) have been observed in the  $N = Z$  nucleus  $^{94}\text{Ag}$ . After beta-delayed  $\gamma$ -ray and proton studies of the isomeric states in  $^{94}\text{Ag}$  performed at GSI [66,67,74,75], direct one-proton decay from the ( $21^+$ ) state to the high-spin states in  $^{93}\text{Pd}$  was observed by detecting protons in coincidence with  $\gamma - \gamma$  correlations and applying  $\gamma$  gates based on the known  $^{93}\text{Pd}$  levels [76]. A year later also direct two-proton radioactivity was observed from the ( $21^+$ ) isomer by detecting fourfold coincidences between proton-proton coincidences measured with the Si detectors and  $\gamma\gamma$  coincidences measured with the Ge detectors at GSI [77]. The  $\gamma - \gamma$  gates were set to two  $\gamma$ -transitions in the daughter nucleus  $^{92}\text{Rh}$ . A two-proton energy of 1900(100) keV [77], an excitation energy of 5780(30) keV [76], and a half-life of 0.39(4) s [75] has been obtained for this ( $21^+$ ) isomer.

At JYFLTRAP, we have measured the mass excesses of  $^{92}\text{Rh}$  and  $^{94}\text{Pd}$  [51], the two-proton-decay daughter of the ( $21^+$ ) isomer, and the beta-decay daughter of  $^{94}\text{Ag}$ , respectively. The mass of  $^{94}\text{Ag}$  was not directly measured but it was extrapolated to  $-53330(360)$  keV based on the linear behaviour of the Coulomb displacement energies of odd-odd  $N = Z$  nuclei [78]. The extrapolated mass of  $^{94}\text{Ag}$  yields a two-proton separation energy  $S_{2\text{p}} = -\Delta(^{94}\text{Ag}) + \Delta(^{92}\text{Rh}) + 2\Delta(^1\text{H}) = 4910(360)$  keV [78], where  $\Delta$  refers to the mass excess. If this value is now combined with the two-proton decay data [77], an excitation energy of 8360(370) keV [78] is obtained for the ( $21^+$ ) state.

The one-proton decay daughter  $^{93}\text{Pd}$  was not measured directly at JYFLTRAP. Instead, two-proton separation energies of several  $N = 47$  isotones have been determined at JYFLTRAP. A parabolic fit to the smooth behaviour of these  $S_{2\text{p}}$  values yields  $S_{2\text{p}} = 5780(160)$  keV [78] for  $^{93}\text{Pd}$ . Since the mass excess of  $^{91}\text{Ru}$  has been measured

at JYFLTRAP, we obtain from the  $S_{2p}(^{93}\text{Pd})$  value a mass excess of  $-59440(160)$  keV for  $^{93}\text{Pd}$ . Finally, we can calculate the proton separation energy of  $^{93}\text{Pd}$  with the mass of  $^{92}\text{Rh}$  measured at JYFLTRAP,  $S_p(^{93}\text{Pd}) = 3730(160)$  keV [78]. From the mass excesses of  $^{93}\text{Pd}$  and  $^{94}\text{Ag}$ , a proton separation energy of  $1180(390)$  keV [78] is obtained for  $^{94}\text{Ag}$ . If we now combine this value with the one-proton decay data [76], we obtain an excitation energy of  $6960(400)$  keV [78] for the  $(21^+)$  isomer. This disagrees with the value based on the two-proton decay data and suggests that either the one-proton or two-proton decay data of the  $(21^+)$  state in  $^{94}\text{Ag}$  needs revision.

The two-proton decay of the  $(21^+)$  isomer in  $^{94}\text{Ag}$  has raised a lot of discussion recently. Shell-model calculations using a *gds* model space have shown that the additional binding energy due to the large attractive *pn* interaction in the  $0g_{9/2}$  orbit lowers the energy of the  $21^+$  state primarily but the level inversion is caused eventually by the mixing with the  $1d_{5/2}$  configurations [79]. The *gds* shell-model calculations [79] do not support strong deformation for the  $21^+$  state in contrast to Ref. [77], where strong prolate deformation was suggested to explain the unexpectedly high two-proton decay probability [77]. In addition, recent calculations based on statistical theory of hot rotating nucleus combined with the macroscopic-microscopic approach do not support a strong prolate deformation [80].

The direct two-proton decay has been questioned in many papers. For example, the level scheme of  $^{92}\text{Rh}$  has been improved from Ref. [81]: the tentative 575-keV  $\gamma$ -transition [81] was not observed, the 307-keV transition was assigned as the  $20^{(-)} \rightarrow 19^{(-)}$  transition, the 632-keV  $\gamma$ -rays as the  $19^{(-)} \rightarrow 18^{(-)}$  transition and the order of the 939- and 1034-keV transitions was reversed [82]. No  $\gamma$ -rays at energies at 565 and 833 keV in coincidence with the known  $\gamma$ -transitions in  $^{92}\text{Rh}$  were observed in Ref. [82] in contrast to Ref. [77]. The data of Ref. [82] suggest that the spin difference between the two-proton decay mother and daughter should be greater than 10 and that the isomer should be even more deformed. When the in-beam data of Ref. [82] is combined with the (extrapolated) mass excess data of AME03 [43], the two-proton decay scenario seems to be impossible. Later, these considerations have been discussed in Refs. [83,84].

Protons could not be unambiguously identified in Ref. [77] since two 1-mm thick Si detectors, which are also sensitive to electrons and positrons, were used. Detailed discussion in Ref. [85] shows that the 1.9-MeV two-proton peak could originate from Compton-scattered  $\gamma$ -rays following the beta decay of the  $7^+$  isomer in  $^{94}\text{Ag}$  and annihilation radiation, and not from  $^{92}\text{Rh}$ . However, these considerations are based on the assumption that Compton scattering events between adjacent Ge crystals had not been reduced in Ref. [77]. In a recent paper [86], it is clarified that the Compton scattering effects in  $\gamma - \gamma$  coincidence events were reduced by excluding double hits in adjacent Ge crystals while they were accepted in the other crystals [67,86]. In addition, the coincidence events with the sum energy of the two  $\gamma$ -rays corresponding to  $511 \pm 1.5$  keV were excluded for all crystals [86].

To identify the protons from the  $21^+$  isomer in  $^{94}\text{Ag}$ , a measurement employing an array of 24  $\Delta E1(\text{gas})$ - $\Delta E2(\text{gas})$ - $E(\text{Si})$  detectors was performed at Lawrence Berkeley National Laboratory [87]. There, the total two-proton coincidence yield for the used reaction of 197-MeV  $^{40}\text{Ca}$  beam on  $^{58}\text{Ni}$  target should have been comparable to the yield at GSI. However, only the lower energy one-proton decay group at 0.79(3) MeV with its branching ratio of 1.9(5) % was confirmed [87]. No evidence for the direct two-proton decay was found [87]. Thus, Ref. [87] suggests that the one-proton decay data should be correct and we should adopt the excitation energy of  $6960(400)$  keV [78] for the  $(21^+)$  isomer.

At IGISOL, developments to produce  $^{94}\text{Ag}$  continue [88,89]. The hot cavity laser ion source has been successfully commissioned at IGISOL and the laser ionization has been found to be fully saturated [89]. If the tests with stable  $^{107}\text{Ag}^{21+}$  beam from the K-130 cyclotron will be successful, the on-line experiments with  $^{94}\text{Ag}$  will be carried out at IGISOL. In future, the mass measurements of the ground and isomeric states of  $^{94}\text{Ag}$  with JYFLTRAP Penning trap mass spectrometer would solve the two-proton decay energy puzzle. The measurement of the hyperfine structure of the isomeric states would experimentally determine the spectroscopic quadrupole moment, and thus, also the shape of the isomer.

### 4.3 $^{95}\text{Pd}^m$

The  $(21/2^+)$  isomer in  $^{95}\text{Pd}$  with a half-life of 13.3(3) s [90] was first observed at Munich MP tandem via beta-delayed proton and gamma spectroscopy [69]. The total beta branching to proton-emitting states was determined as 0.74(19) %. The final state to be populated after the beta decay was found to be  $8^+$  in  $^{94}\text{Ru}$ . The most strongly populated level in the beta decay of  $^{95}\text{Pd}^m$  was the  $(21/2^+)$  level at 2449 keV in  $^{94}\text{Rh}$ . Soon after this experiment, the known properties of  $^{95}\text{Pd}$  were confirmed at GSI [90]. Shell-model calculations [91] suggest that this isomer lies at 1.90 MeV and is a spin-gap isomer in nature. Other shell-model calculations have predicted excitation energies of 1803 keV [92,93] and 1973 keV [94] for this spin-gap isomer. The extrapolated value in the AME03 is  $1860(500)\#$  keV [43]. The energy of the isomeric state was experimentally determined as 1876 keV [68] based on the  $\gamma$  transitions connecting the states built on the ground and isomeric states of  $^{95}\text{Pd}$ .

At JYFLTRAP, a 170-MeV  $^{40}\text{Ca}$  beam on a  $^{nat}\text{Ni}$  target was used for the production of the ground and isomeric states of  $^{95}\text{Pd}$  [51]. For these rather long-lived states with an energy difference of about 2 MeV, a quadrupole RF excitation time of 800 ms in the precision trap allowed separate mass measurements for the ground and isomeric state. The reference ion used in these measurements was  $^{94}\text{Mo}$ . The measured mass excesses for the ground and isomeric state of  $^{95}\text{Pd}$  were  $-69961.6(4.8)$  keV and  $-68086.2(4.7)$  keV [51], respectively. This yields an excitation energy of  $1875.4(6.7)$  keV [51] for the  $(21/2^+)$  isomer in  $^{95}\text{Pd}$  in agreement with the result of Ref. [68]. It

further confirms the spin-gap character of the transition as the  $21/2^+$  state lies lower in energy than the  $15/2^+$  (1973 keV) and  $17/2^+$  (1879 keV) states [68]. A recent mass measurement of the reference  $^{94}\text{Mo}$  against  $^{85}\text{Rb}$  has shown that the mass excess of  $^{94}\text{Mo}$  is off by  $-3.0(21)$  keV. This has an effect on the mass-excess values of the ground and isomeric states but does not change the value for the excitation energy of the isomer.

The obtained  $Q_{\text{EC}}$  value for the isomer,  $10256.1(6.3)$  keV [51], together with the branching ratio of 35.8 % [90] for the beta decay to the ( $21/2^+$ ) state at 2449 keV in  $^{94}\text{Rh}$ , yields a  $\log ft = 5.5$  for this most dominant beta transition. This confirms the allowed character of the transition. The measurement of the mass of  $^{95}\text{Pd}^{\text{m}}$  was the first direct Penning trap mass measurement of a high-spin isomer and it proved that JYFLTRAP can also be used for the studies of spin-gap isomers.

## 5 Conclusions and Outlook

The studies of neutron-deficient nuclides at the  $rp$ -process path have been an important part of the physics performed at IGISOL. Decay studies and  $Q_{\text{EC}}$ -value measurements of the mirror beta decays as well as the studies of the  $T = 1$  triplet at  $A = 58$  with the light-ion guide have yielded information necessary for precise and corrected  $ft$  values and for the studies of the isospin symmetry of transitions. The IGISOL method has shown its strength in the production of Y, Nb and Zr isotopes. JYFLTRAP Penning trap mass spectrometer has been employed for  $Q_{\text{EC}}$ -value measurements as well as for measuring the masses or excitation energies of the long-lived isomers, such as  $^{53}\text{Co}^{\text{m}}$  and  $^{95}\text{Pd}^{\text{m}}$ .

By combining the latest state-of-the-art detectors for spectroscopy experiments and employing JYFLTRAP for isobaric purification, many of the older experiments performed with He-jet or IGISOL techniques could be superseded in future. Other future challenges are for example the identification of isomeric and ground states in the mass  $A = 80 - 90$  region via post-trap spectroscopy. Since the states are populated differently in the heavy-ion and light-ion fusion-evaporation reactions, some isomeric states, such as  $^{93}\text{Ru}^{\text{m}}$  or  $^{91}\text{Tc}^{\text{m}}$ , could also be produced with the light-ion ion guide method similarly to the earliest studies of these isomers. There are still many open questions in this mass region, such as the observed  $\gamma$ -rays at  $A = 85$ , and the excitation energies of  $^{85}\text{Nb}^{\text{m}}$ ,  $^{86}\text{Nb}^{\text{m}}$  and  $^{94}\text{Ag}^{\text{m}}$ . For the production of  $^{94}\text{Ag}^{\text{m}}$  ( $21^+$ ) isomer, the development and testing of the hot-cavity laser ion source at IGISOL are essential.

Spectroscopic experiments provide information on the ground, excited and isomeric states (spins, energies, half-lives), and possible decay modes of the studied nuclides. These data are relevant for the  $rp$  and recently proposed  $\nu p$  process [95] network calculations, which should also take into account the contribution from the isomers. Close collaboration with nuclear astrophysicists modeling the  $rp$  and  $\nu p$  processes will continue in future. It would be beneficial to establish a large campaign to measure the interest-

ing spectroscopic details within the relevant mass region at the new IGISOL4 facility in collaboration with the  $rp$  and  $\nu p$  process modelers. In this way, the impact of new data on the modeling of the  $rp$  or  $\nu p$  processes would be seen immediately.

This work has been supported by the Academy of Finland under the Finnish Centre of Excellence Programme 2006-2011 (Nuclear and Accelerator Based Physics Programme at JYFL). The support via the Finnish-Russian Interacademy Agreement (project No. 8) is acknowledged. A.K. acknowledges the support from the Academy of Finland under the project 127301.

## References

1. J. Honkanen, Ph.D. thesis, Department of Physics, University of Jyväskylä, 1981.
2. J. Honkanen *et al.*, Phys. Scr. **19**, 239 (1979).
3. J. Honkanen *et al.*, Nucl. Phys. A **330**, 429 (1979).
4. K. Eskola *et al.*, Nucl. Phys. A **341**, 365 (1980).
5. J. Honkanen *et al.*, Nucl. Phys. A **380**, 410 (1982).
6. J. Honkanen *et al.*, Nucl. Phys. A **471**, 489 (1987).
7. J. Honkanen, M. Kortelahti, K. Eskola, and K. Vierinen, Nucl. Phys. A **366**, 109 (1981).
8. J. Ärje *et al.*, Phys. Rev. Lett. **54**, 99 (1985).
9. J. Äystö *et al.*, Phys. Lett. B **138**, 369 (1984).
10. M. Oinonen *et al.*, Nucl. Instrum. Methods Phys. Res. A **416**, 485 (1998).
11. J. Huikari *et al.*, Nucl. Instrum. Methods Phys. Res. B **222**, 632 (2004).
12. R. Wallace and S. E. Woosley, Astrophys. J. Suppl. Ser. **45**, 389 (1981).
13. H. Schatz *et al.*, Phys. Rep. **294**, 167 (1998).
14. Y. Sun, M. Wiescher, A. Aprahamian, and J. Fisker, Nucl. Phys. A **758**, 765 (2005).
15. H. Schatz and K. Rehm, Nucl. Phys. A **777**, 601 (2006).
16. H. Schatz *et al.*, Phys. Rev. Lett. **86**, 3471 (2001).
17. V.-V. Elomaa *et al.*, Phys. Rev. Lett. **102**, 252501 (2009).
18. A. Kankainen *et al.*, Phys. Rev. C **82**, 034311 (2010).
19. A. Kankainen, A. Honkanen, K. Peräjärvi, and A. Saastamoinen, Hyperfine Interact. (2012).
20. G. Martínez-Pinedo, A. Poves, E. Caurier, and A. P. Zuker, Phys. Rev. C **53**, R2602 (1996).
21. B. H. Wildenthal, M. S. Curtin, and B. A. Brown, Phys. Rev. C **28**, 1343 (1983).
22. H. Fujita *et al.*, Phys. Rev. C **75**, 034310 (2007).
23. K. Peräjärvi *et al.*, Nucl. Phys. A **696**, 233 (2001).
24. Z. Janas *et al.*, Eur. Phys. J. A **12**, 143 (2001).
25. H. Jongsma, A. D. Silva, J. Bron, and H. Verheul, Nucl. Phys. A **179**, 554 (1972).
26. J. M. Freeman *et al.*, Nucl. Phys. **69**, 433 (1965).
27. A. Kankainen *et al.*, Eur. Phys. J. A **25**, 129 (2005).
28. A. Jokinen *et al.*, Eur. Phys. J. A **3**, 271 (1998).
29. L. M. Fraile and J. Äystö, Nucl. Instrum. Methods Phys. Res. A **513**, 287 (2003).
30. A. Kankainen, Ph.D. thesis, Department of Physics, University of Jyväskylä, 2006.
31. Y. Novikov *et al.*, Eur. Phys. J. A **11**, 257 (2001).
32. J. Parmonen *et al.*, Nucl. Instrum. Methods Phys. Res. A **306**, 504 (1991).
33. A. Piechaczek *et al.*, Phys. Rev. C **61**, 047306 (2000).

34. J. Döring *et al.*, Phys. Rev. C **57**, 1159 (1998).
35. J. J. Ressler *et al.*, Phys. Rev. Lett. **84**, 2104 (2000).
36. J. Döring *et al.*, Phys. Rev. C **59**, 59 (1999).
37. A. Kankainen *et al.*, Eur. Phys. J. A **25**, 355 (2005).
38. C. J. Lister, P. E. Haustein, D. E. Alburger, and J. W. Olness, Phys. Rev. C **24**, 260 (1981).
39. S. Della Negra, H. Gauvin, D. Jacquet, and Y. Le Beyec, Z. Phys. A **307**, 305 (1982).
40. S. Mitarai *et al.*, Nucl. Phys. A **557**, 381 (1993).
41. C. M. Baglin, Nucl. Data Sheets **109**, 2257 (2008).
42. A. Kankainen *et al.*, Eur. Phys. J. A **29**, 271 (2006).
43. G. Audi, A. H. Wapstra, and C. Thibault, Nucl. Phys. A **729**, 337 (2003).
44. R. Iafigliola and J. K. P. Lee, Phys. Rev. C **13**, 2075 (1976).
45. W. X. Huang *et al.*, Phys. Rev. C **59**, 2402 (1999).
46. T. Kuroyanagi *et al.*, Nucl. Phys. A **484**, 264 (1988).
47. D. Bucurescu *et al.*, Z. Phys. A **342**, 403 (1992).
48. T. Shizuma *et al.*, Z. Phys. A **348**, 25 (1994).
49. R. Iafigliola, S. C. Gujrathi, B. L. Tracy, and J. K. P. Lee, Can. J. Phys. **52**, 96 (1974).
50. K. Oxorn and S. K. Mark, Z. Phys. A **303**, 63 (1981).
51. C. Weber *et al.*, Phys. Rev. C **78**, 054310 (2008).
52. D. Rudolph *et al.*, Phys. Rev. C **47**, 2574 (1993).
53. S. Dean *et al.*, Eur. Phys. J. A **21**, 243 (2004).
54. E. Browne, Nucl. Data Sheets **82**, 379 (1997).
55. G. Gräff, H. Kalinowsky, and J. Traut, Z. Phys. A **297**, 35 (1980).
56. M. König *et al.*, Int. J. Mass Spectrom. Ion Processes **142**, 95 (1995).
57. A. Kellerbauer *et al.*, Eur. Phys. J. D **22**, 53 (2003).
58. R. T. Birge, Phys. Rev. **40**, 207 (1932).
59. V.-V. Elomaa *et al.*, Nucl. Instrum. Methods Phys. Res. A **612**, 97 (2009).
60. T. Eronen *et al.*, Phys. Rev. Lett. **100**, 132502 (2008).
61. J. Äystö *et al.*, Nucl. Phys. A **404**, 1 (1983).
62. J. C. de Lange *et al.*, Z. Phys. A **279**, 79 (1976).
63. D. F. Geesaman *et al.*, Phys. Rev. Lett. **34**, 326 (1975).
64. K. Eskola, Phys. Lett. **23**, 471 (1966).
65. K. Jackson *et al.*, Phys. Lett. B **33**, 281 (1970).
66. M. L. Commara *et al.*, Nucl. Phys. A **708**, 167 (2002).
67. C. Plettner *et al.*, Nucl. Phys. A **733**, 20 (2004).
68. N. Märginean *et al.*, Phys. Rev. C **67**, 061301 (2003).
69. E. Nolte and H. Hick, Z. Phys. A **305**, 289 (1982).
70. I. Perlman *et al.*, Phys. Rev. **127**, 917 (1962).
71. J. Cerny, J. Esterl, R. Gough, and R. Sextro, Phys. Lett. B **33**, 284 (1970).
72. J. Cerny, R. A. Gough, R. G. Sextro, and J. E. Esterl, Nucl. Phys. A **188**, 666 (1972).
73. D. Mueller, E. Kashy, W. Benenson, and H. Nann, Phys. Rev. C **12**, 51 (1975).
74. K. Schmidt *et al.*, Z. Phys. A **350**, 99 (1994).
75. I. Mukha *et al.*, Phys. Rev. C **70**, 044311 (2004).
76. I. Mukha *et al.*, Phys. Rev. Lett. **95**, 022501 (2005).
77. I. Mukha *et al.*, Nature **439**, 298 (2006).
78. A. Kankainen *et al.*, Phys. Rev. Lett. **101**, 142503 (2008).
79. K. Kaneko, Y. Sun, M. Hasegawa, and T. Mizusaki, Phys. Rev. C **77**, 064304 (2008).
80. M. Aggarwal, Phys. Lett. B **693**, 489 (2010).
81. D. Kast *et al.*, Z. Phys. A **356**, 363 (1997).
82. O. L. Pechenaya *et al.*, Phys. Rev. C **76**, 011304 (2007).
83. I. Mukha, H. Grawe, E. Roeckl, and S. Tabor, Phys. Rev. C **78**, 039803 (2008).
84. O. L. Pechenaya *et al.*, Phys. Rev. C **78**, 039804 (2008).
85. D. G. Jenkins, Phys. Rev. C **80**, 054303 (2009).
86. I. Mukha, E. Roeckl, H. Grawe, and S. Tabor, arXiv:1008.5346v1 [nucl-ex] (2010).
87. J. Cerny *et al.*, Phys. Rev. Lett. **103**, 152502 (2009).
88. T. Kessler *et al.*, Nucl. Instrum. Methods Phys. Res. B **266**, 4420 (2008).
89. M. Reponen *et al.*, Eur. Phys. J. A **42**, 509 (2009).
90. W. Kurcewicz *et al.*, Z. Phys. A **308**, 21 (1982).
91. K. Ogawa, Phys. Rev. C **28**, 958 (1983).
92. S. E. Arnell *et al.*, Phys. Rev. C **49**, 51 (1994).
93. J. Sinatkas, L. D. Skouras, D. Strottman, and J. D. Vergados, J. Phys. G **18**, 1401 (1992).
94. K. Schmidt *et al.*, Nucl. Phys. A **624**, 185 (1997).
95. C. Fröhlich *et al.*, Phys. Rev. Lett. **96**, 142502 (2006).